ELSEVIER

Journal of Photochemistry and Photobiology A: Chemistry 122 (1999) 87–94

Journal of Photochemistry and Photobiology A:Chemistry

Electron-transfer pathway for photoinduced Diels–Alder cycloadditions

Duoli Sun, Stephan M. Hubig, Jay K. Kochi*

Department of Chemistry, University of Houston, Houston, TX 77204-5641, USA

Received 8 October 1998; accepted 21 December 1998

Abstract

The photoinduced [4 + 2] cycloadditions of anthracene to maleic anhydride and various maleimides yield the Diels–Alder adducts in high (chemical) yields. Analysis of the efficiency of these photoreactions as a function of the dienophile concentration leads to limiting quantum efficiencies of $\Phi = 0.014$ and $\Phi = 0.16$ for maleic anhydride and *N*-(pentafluorophenyl)maleimide, respectively. Picosecond time-resolved spectroscopy reveals the one-electron transfer from excited (singlet) anthracene to the dienophile acceptor (resulting in the formation of anthracene cation radical and dienophile anion radical) as the critical step prior to cycloaddition. Competition between coupling, back-electron transfer and dissociation of the ion-radical pair which depends on the solvent polarity and the presence of added (inert) salt, limits the quantum yields of adduct formation.

Keywords: Photoinduced Diels-Alder; Electron-transfer quenching; Solvent-dependent quantum yields; Fluorescence; Picosecond absorption spectroscopy

1. Introduction

Photoinduced Diels–Alder reactions are attainable either by irradiation of photosensitizers (such as ketones) [1–9] or by direct photoactivation of the diene or dienophile [5–16]. Synthetically, such [4 + 2] photocycloadditions have been employed (i) to efficiently prepare exo-adducts that are not readily available by thermal Diels–Alder reaction [1–4,15], (ii) to obtain thermally labile cycloadducts [5–9,13,14], or (iii) to access cyclic azo compounds which serve as precursors for novel biradicals [5–9]. Most importantly, these photoreactions occur with quantum efficiencies as high as $\Phi = 0.6$ [5,6], despite the fact that (concerted) photochemical [4 + 2] cycloadditions are symmetry-forbidden according to the Woodward–Hoffmann rules [17–19]. Thus, [4 + 2] photocycloadditions have been treated on the basis of MO theory by considering a polar (excited) complex between the electron-rich diene and the electron-poor dienophile as intermediate prior to coupling [20–23].

In *thermal* Diels–Alder reactions, electron donor-acceptor (EDA) complexes between dienes and dienophiles are frequently observed as (ground-state) transients [24–27], and in some cases ion radicals have been observed by ESR spectroscopy [28,29]. Moreover, the quantitative comparison of the Diels–Alder cycloaddition of anthracene to tetracyanoethylene (TCNE) with the alkylmetal insertion reactions of TCNE under the same conditions points to a (unifying) electron-transfer mechanism for both reactions [25]. However, the general applicability of an electron-transfer pathway for thermal Diels–Alder reactions has remained controversial [25,26,28,29]. The majority of *photoinduced* Diels–Alder reactions clearly involve electron donors and acceptors as diene and dienophile, respectively [1–16], and EDA complexes [5–10] (in the ground state) as well as excited charge-transfer complexes (exciplexes) [13,14,30] have been observed by absorption and emission spectroscopy, respectively. Although these findings together with the theoretical postulate of a polar intermediate complex (vide supra) point quite inevitably to an electron-transfer pathway for photoinduced Diels–Alder reactions, no direct (experimental) evidence for such a mechanism has been hitherto reported.

In this study, we investigate the photoinduced [4 + 2] cycloaddition of anthracene to dienophiles such as maleic anhydride [10] and the related maleimides in Chart I.

*Corresponding author.

1010-6030/99/$ – see front matter
PII: S1010-6030(99)00007-6

Chart I

Dienophiles:

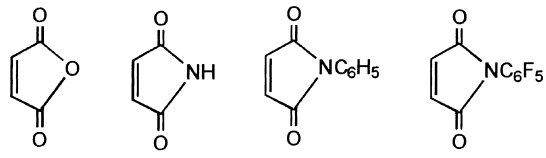

MA **MI** **PMI** **PFMI**

Diels-Alder Products:

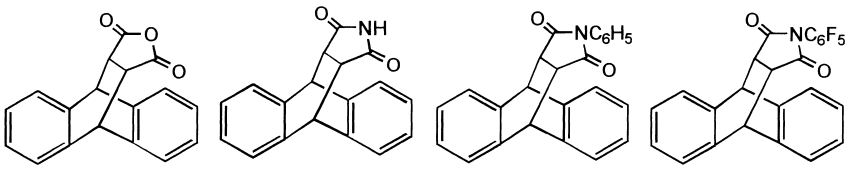

1 **2** **3** **4**

Steady-state and time-resolved photochemical techniques, such as fluorescence measurements and picosecond laser photolysis experiments, reveal one-electron transfer from the excited (singlet) anthracene to the dienophile as the first reaction step towards [4 + 2] cycloaddition. Further evidence for the proposed electron-transfer mechanism is provided by the effects of quencher concentration, solvent, and added inert salt on the photochemical quantum yields of the formation of the Diels–Alder adducts in Chart I.

2. Experimental

2.1. Materials and methods

Anthracene, maleimide, and *N*-ethylmaleimide from Aldrich were used as received. *N*-phenylmaleimide and *N*-(pentafluorophenyl) maleimide were prepared via the reaction of the corresponding aniline with maleic anhydride [31]. Maleic anhydride, acetonitrile, dichloromethane, benzene, toluene, *p*-xylene, tetrahydrofuran, and dioxane were purified according to published procedures [32]. Melting points were measured on a MEL-TEMP apparatus and are uncorrected. ^{1}H NMR spectra were recorded in $CDCl_3$ on a General Electric QE-300 NMR spectrometer and the chemical shifts are reported in ppm units downfield from internal tetramethylsilane. UV–Vis absorption and Infrared spectra were recorded on a Hewlett-Packard 8453 diode-array spectrometer and a Nicolet 10 DX FT spectrometer, respectively. Fluorescence measurements were carried out on a Perkin Elmer Luminescence Spectrometer LS 50. Gas chromatography was performed on a Hewlett-Packard 5890A gas chromatograph equipped with a HP 3392 integrator. GC-MS analyses were carried out on a Hewlett-Packard 5890 gas chromatograph interfaced to a HP 5970 mass spectrometer (EI, 70 eV). HPLC analyses were performed on an LDC Analytical instrument (SM 3100) equipped with a Hypersil BDS C18 reverse-phase column (20 cm) with acetonitrile/water mixtures as eluent. All chemical analyses were carried out by Atlantic Microlab, Norcross, GA.

2.2. Photoinduced Diels–Alder reaction of anthracene with maleic anhydride and maleimides

General procedure for the preparative photolysis: To a solution of maleic anhydride (0.4 mmol, 0.04 M) in chloroform under an argon atmosphere was added 0.6 mmol of anthracene in small portions[1] while the solution was irradiated with a focused beam from a medium pressure mercury lamp (500 W) passed through an aqueous IR filter and an ESCO 340 nm sharp cut-off filter. Under these experimental conditions, only anthracene and not maleic anhydride absorbed the actinic light. The photoreaction was carried out until HPLC analysis showed that most (>90%) of the maleic anhydride was consumed, and the Diels–Alder product was formed in >95% yield. After filtration, the solvent was evaporated and the crude product was washed with hexane and then recrystallized from toluene. The Diels–Alder adduct **1** was isolated, purified by recrystallization from toluene, and identified by comparison of the spectral data with those of the thermal product. Similar procedures were used for the Diels–Alder reactions with the

[1]The purpose of this procedure was to reduce the competing anthracene dimerization and thus to facilitate the workup procedure.

maleimides in Chart I and the characteristic physical data for all Diels–Alder adducts (**1**–**4**) are as follows: Anthracene-9, 10-endo-α, β-succinic anhydride **1**: mp > 250°C (lit. 256–260°C) [33]; IR (cm^{-1}): 2973, 2367, 2338, 1865, 1787, 1460, 1230, 1211, 1072, 975, 926, 842, 757, 715, 703, 636, 612, 539, 412; ^{1}H NMR ($CDCl_3$): δ, 7.14–7.37 (m, 8H), 4.79 (s, 2H), 3.50 (s, 2H); *Anal.* Calc. for $C_{18}H_{12}O_3$: C, 78.26; H, 4.35. Found: C, 78.39; H, 4.49%. Anthracene-9, 10-endo-α, β-succinimide **2**: mp > 250°C (lit. 303–304°C) [34]; IR (cm^{-1}): 2929, 2853, 2365, 2340, 1786, 1730, 1466, 1339, 1319, 1182, 1162, 1157, 989, 959, 806, 786, 771, 684, 663, 608, 532; ^{1}H NMR ($CDCl_3$): 7.11–7.35 (m, 8H), 4.73 (s, 2H), 3.22 (s, 2H); *Anal.* Calc. for $C_{18}H_{13}NO_2$: C, 78.55; H, 4.73. Found: C, 78.60; H, 4.69%. Anthracene-9, 10-endo-α, β-*N*-phenylsuccinimide **3**: mp 201–202°C (lit. 203°C) [35]; IR (cm^{-1}): 2961, 2368, 2344, 1774, 1712, 1496, 1466, 1387, 1199, 1175, 1024, 921, 886, 830, 763, 751, 721, 697, 636, 624, 557; ^{1}H NMR ($CDCl_3$): δ, 7.18–7.40 (m, 13H), 4.86 (s, 2H), 3.34 (s, 2H); *Anal.* Calc. for $C_{24}H_{17}NO_2$: C, 82.05; H, 4.84. Found: C, 82.05; H, 4.96%. Anthracene-9, 10-endo-α, β-*N*-(pentafluorophenyl)succinimide **4**: mp > 250°C; IR (cm^{-1}): 2961, 2362, 1738, 1526, 1466, 1363, 1302, 1181, 1145, 999, 781, 757, 603, 551; ^{1}H NMR ($CDCl_3$): δ, 7.20–7.42 (m, 8H), 4.88 (s, 2H), 3.47 (s, 2H); *Anal.* Calc. for $C_{24}H_{12}NF_5O_2$: C, 65.31; H, 2.72. Found: C, 65.44; H, 2.83%.

2.3. Determination of quantum yields for the photocycloaddition of anthracene to maleic anhydride and maleimides

The quantum yields were measured with the aid of a medium-pressure (500 W) mercury lamp focused through an aqueous IR filter followed by an ESCO 340 nm cut-off filter. The intensity of the lamp at $\lambda = 365$ nm was determined with a freshly prepared potassium ferrioxalate actinometer solution [36,37] in a 1 cm cuvette fitted with a Schlenk adapter. The absorbance at $\lambda = 365$ nm of a solution of anthracene (0.01 M) and maleic anhydride (0.02 M) in chloroform remained above 1.5 throughout the irradiation, and thus no correction for transmitted light was necessary. A 50 μl aliquot was taken, diluted with 2 ml of acetonitrile, and the content quantified by HPLC using benzophenone as an internal standard. The quantum efficiencies for the formation of the Diels–Alder adduct and anthracene dimer as well as for the anthracene consumption are listed in Table 1.

2.4. Fluorescence measurements

Solutions of 0.0006 M anthracene and 0–0.1 M maleic anhydride or *N*-(pentafluorophenyl)maleimide in chloroform were prepared in 1 cm quartz cuvettes. The fluorescence spectra were measured from 390 to 590 nm at room temperature using a Perkin Elmer Luminescence Spectrometer LS 50. All samples were excited at 358 nm, and the fluorescence intensities were determined at 403 nm and 427 nm.

Table 1
Quantum yields for the photoinduced Diels–Alder addition of anthracene to maleic anhydride and maleimide dienophiles (DP)[a]

DP[b]	Φ_{ANT}[c]	Φ_{D-A}[d]	Φ_{dim}[e]
MA	0.013	0.009	0.002
MI	0.051	0.040	0.005
PMI	0.038	0.031	0.004
PFMI	0.11	0.095	0.006

[a] 0.01 M ANT and 0.02 M DP in chloroform irradiated at −30°C with a medium pressure Hg lamp with 340 nm cutoff filter.
[b] Identified in Chart I.
[c] Quantum yields for anthracene consumption.
[d] Quantum yields for Diels–Alder-adduct formation.
[e] Quantum yields for anthracene dimerization as determined by ferrioxalate actinometry.

2.5. Time-resolved (ps) absorption measurements

The picosecond time-resolved absorption measurements were carried out with a kinetic spectrometer and a mode-locked (25 ps) Nd:YAG laser using the third harmonic output at 355 nm (10 mJ per pulse) for the excitation of anthracene [38]. The solutions of anthracene and maleic anhydride were prepared under an argon atmosphere in a 1 cm cuvette fitted with a Schlenk adapter. The concentration of anthracene was adjusted for absorbances in the range 1.0–1.5 at the excitation wavelength ($\lambda_{exc} = 355$ nm), and the concentration of maleic anhydride was varied between 0.1 and 0.5 M.

3. Results

3.1. Photoinduced [4 + 2] cycloaddition of anthracene to maleic anhydride and maleimides

An equimolar (0.04 M) solution of anthracene (ANT) and maleic anhydride (MA) in chloroform was irradiated with ultraviolet light from a medium-pressure mercury lamp ($\lambda_{irr.} > 340$ nm) at −30°C. Under these conditions, the thermal Diels–Alder reaction was completely suppressed and more than 90% of the incident light ($\lambda_{irr.} = 365$ nm) was absorbed by anthracene as confirmed by UV–Vis spectroscopy[2]. Periodic HPLC analysis of the photolysate revealed the simultaneous disappearance of ANT and MA, and the monotonic appearance of a single product. After prolonged (ca. 100 h) irradiation, the HPLC analysis showed 97% consumption of maleic anhydride and 95% formation of the Diels–Alder product. The Diels–Alder adduct **1** was isolated and identified by comparison of the NMR and IR

[2] CT absorption of the electron donor–aceptor complex of anthracene with maleic anhydride [10] could be neglected under these conditions.

spectral data with those of the thermal Diels–Alder product. Photoreactions of anthracene with the other dienophiles in Chart I were carried out in a similar way, and the spectral data of all photoproducts are given in Section 2.

3.2. Quantum efficiencies for the photocycladdition of anthracene to maleic anhydride and maleimides

For the determination of the quantum yields, the photoinduced Diels–Alder reactions were carried out with monochromatic light at $\lambda_{irr.} = 365$ nm, and the intensity of the light source was measured by ferrioxalate actinometry [36,37]. Photocycloaddition of maleic anhydride to anthracene was found to be a rather inefficient process with $\Phi_{D-A} \cong 1\%$ (see Table 1). By contrast, the photoreaction of anthracene with the other dienophiles in Chart I afforded better quantum efficiencies with $\Phi_{D-A} = 3$–10% (entries 2–4 in Table 1). In all cases, anthracene dimerization leading to the [4 + 4] cycloadduct was also observed, however with very low quantum yields of $\Phi_{dim} \leq 0.006$.

3.3. Effects of dienophile concentration on the quantum efficiencies

The quantum-efficiency (Φ_{D-A}) for the photocycloaddition depended on the concentration of the dienophile [DP] as exemplified for maleic anhydride and *N*-(pentafluorophenyl)maleimide in Table 2. Thus, at low dienophile concentration ([DP] < 0.02 M), Φ_{D-A} increased steadily with [DP]. However, at concentrations of [DP] > 0.02 M, the quantum efficiencies reached a plateau value of 0.013 and 0.110 for maleic anhydride and *N*-(pentafluorophenyl)maleimide, respectively. Such an asymptotic behavior of Φ_{D-A} (see Fig. 1(A)) is commonly evaluated in a double-reciprocal presentation as shown in Fig. 1(B), and the linear plots of $1/\Phi_{D-A}$ versus 1/[DP] gave intercepts of 72.4 and 6.33, and slopes of 0.832 and 0.065 for MA and PFMI, respectively. From the intercepts, limiting quantum yields of $\Phi_{D-A,\infty} = 0.014$ and 0.16 were obtained for MA and PFMI, respectively.

Table 2
Concentration dependence of the quantum efficiencies[a]

[DP][b]	MA[c]		PFMI[c]	
	Φ_{D-A}[d]	Φ_{dim}[e]	Φ_{D-A}[d]	Φ_{dim}[e]
0.0019			0.020	0.044
0.0026			0.028	0.037
0.0029			0.030	0.029
0.0034			0.042	0.031
0.0050	0.0043	0.0040	0.072	0.027
0.012	0.0062	0.0026	0.100	0.016
0.019	0.0090	0.0020	0.095	0.006
0.040	0.011	0	0.104	0.003
0.062	0.012	0	0.110	0.002
0.098	0.013	0		
0.199	0.013	0		

[a] A chloroform solution of 0.01 M anthracene and of varying dienophile concentration was irradiated at $\lambda_{irr.} = 365$ nm at −30°C.
[b] Dienophile concentration.
[c] As identified in Chart 1.
[d] Quantum yields of Diels–Alder-adduct formation.
[e] Quantum yields of anthracene dimerization as determined by ferrioxalate actinometry.

Table 3
Solvent and salt effects on the quantum efficiency of the photoinduced cycloaddition of anthracene to PFMI[a]

No	Solvent	Φ_{D-A}[b]	Φ_{dim}[c]	ε[d]	$E_T(30)$[e]
1	Dioxane	0.11	0.03	2.21	36.0
2	Chloroform	0.10	0.04	4.81	39.1
3	Dichloromethane	0.02	0.03	8.93	40.7
4	Acetonitrile	0.007	0.02	35.9	45.6
5	Chloroform (0.1 M TBA·PF_6)	0.06	0.04		
6	Chloroform (0.5 M TBA·PF_6)	0.03	0.02		

[a] Photoreactions were carried out at room temperature.
[b] Quantum yield of Diels–Alder-adduct formation.
[c] Quantum yield of anthracene dimerization as determined by ferrioxalate actinometry.
[d] Dielectric constant from [39].
[e] Dimroth–Reichardt parameter for solvent polarity from [39].

3.4. Solvent and salt effects

The photoinduced Diels–Alder reaction with PFMI was carried out in various solvents of different polarity. The data in Table 3 (entries 1–4) demonstrate that the quantum yield of Diels–Alder addition (Φ_{D-A}) decreased with increasing dielectric constant (ε) or Dimroth–Reichardt parameter, $E_T(30)$, both of which represent quantitative measurements of the solvent polarity [39]. On the other hand, the quantum yield of anthracene dimerization (Φ_{dim}) remained more or less the same in all four solvents. The presence of tetra-*n*-butylammonium hexafluorophosphate salt in chloroform resulted in quantum efficiencies which decreased by a factor of 2 for 0.1 M salt (compare entries 2 and 5) and a factor of 3 for 0.5 M salt (compare entries 2 and 6).

3.5. Steady-state fluorescence measurements

The fluorescence spectrum of a diluted (ca. 6×10^{-4} M) solution of anthracene in chloroform excited at $\lambda_{exc} = 358$ nm showed the characteristic emission bands of the excited (singlet) anthracene at 403, 427, 455 and 480 nm. Upon incremental addition of the dienophiles MA or PFMI, the intensity of the fluorescence bands decreased steadily reaching negligible values at dienophile concentrations greater than 0.1 M. Thus, the quenching of the fluorescence of anthracene by both dienophiles was evaluated by the Stern–Volmer relationship in Eq. (1), i.e.

$$\frac{I_0}{I} = 1 + k_q \tau_0 [DP] \quad (1)$$

where I and I_0 are the fluorescence intensities in the presence and absence of quencher, respectively, k_q is the second-order

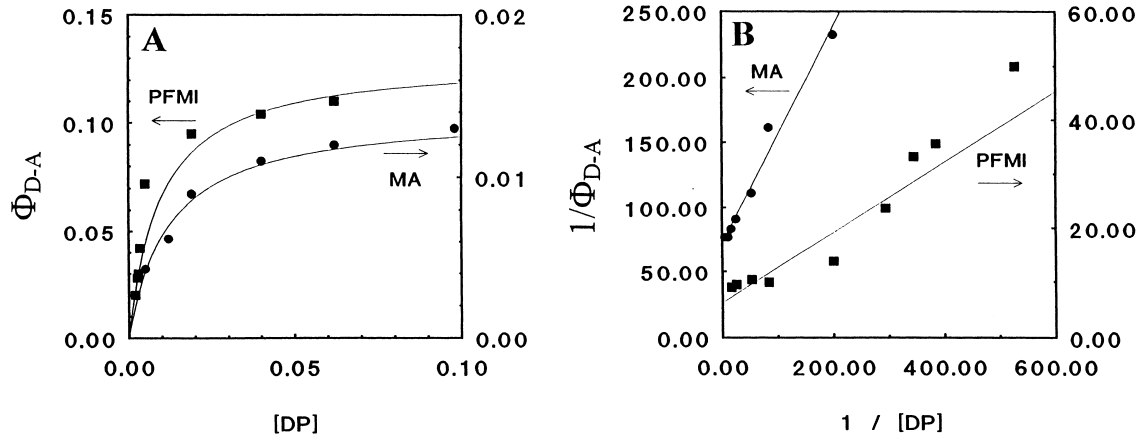

Fig. 1. (A) Asymptotic behavior of the quantum yields for photocycloaddition of anthracene to maleic anhydride (MA) and *N*-(pentafluorophenyl) maleimide (PFMI) vs. dienophile concentration and (B) its double-reciprocal evaluation according to Eq. (8). The concentration dependence in (A) is simulated (solid line) taking the limiting quantum yields and the rate constants extracted from the double-reciprocal plots.

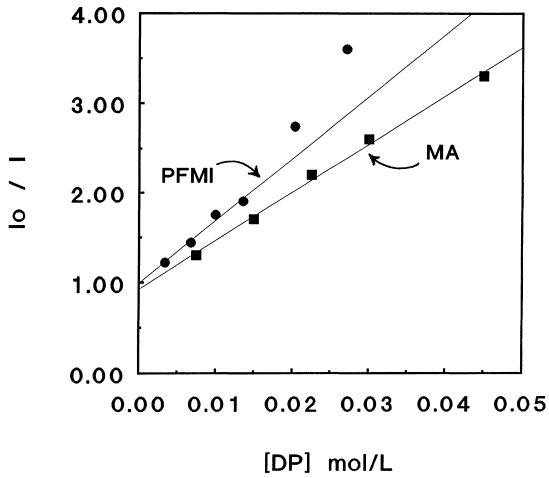

Fig. 2. Stern–Volmer presentation of the (steady-state) fluorescence quenching of anthracene (6×10^{-4} M) by maleic anhydride (MA) and *N*-(pentafluorophenyl) maleimide (PFMI) in chloroform. The upward deviation of the PFMI data from the linear Stern–Volmer relationship is due to (charge-transfer) complex formation in the ground state.

quenching rate constant, τ_0 is the natural lifetime of the excited singlet state of anthracene (in the absence of quencher), and [DP] is the molar concentration of the dienophile quencher. Thus, linear plots of I_0/I versus the dienophile concentration were obtained as shown for maleic anhydride and PFMI in Fig. 2[3]. Accordingly, taking $\tau_0 = 2.1 \times 10^{-9}$ s as singlet lifetime[4], we determined the quenching rate constants of $k_q = 2.5 \times 10^{10}$ and $3.8 \times 10^{10}\ M^{-1}\ s^{-1}$ for MA and PFMI, respectively.

[3]At quencher concentrations higher than 0.02 M for PFMI and 0.05 M for MA, the Stern–Volmer plots showed an upward curvature due to the formation of (ground-state) EDA complexes between anthracene and the dienophiles. For a theoretical treatment of such deviations from the Stern–Volmer reationship see [40].

[4]The lifetime of singlet excited anthracene in chloroform was determined by time-resolved (ps) spectroscopy [vide infra]. For lifetimes in other solvents see [41].

3.6. Time-resolved (ps) spectroscopy of the reactive intermediates in the photoinduced Diels–Alder addition of anthracene to maleic anhydride

To probe the nature of the intermediates formed upon the quenching of excited anthracene by maleic anhydride, a solution of anthracene (0.005 M) and MA (0.3 M) in chloroform was exposed to a 25 ps pulse of a mode-locked Nd : YAG laser at 355 nm [38]. The time-resolved (ps) spectra in Fig. 3(A) show two absorption bands centered at 600 and 720 nm. The 600 nm absorption band with its characteristic fine structure and steep fall-off toward the longer wavelength region was identical with the transient spectrum obtained upon photoexcitation of anthracene in chloroform in the absence of maleic anhydride (see Fig. 3(B)); and it was ascribed to the S_1–S_n absorption band of excited (singlet) anthracene ($^1ANT^*$). The second absorption at 720 nm was assigned to the cation-radical of anthracene ($ANT^{+\bullet}$) [42–44]. The absorption band of $^1ANT^*$ decayed on the picosecond timescale following first-order kinetics with a rate constant of $k_{decay} = 1 \times 10^{10}\ s^{-1}$. This decay rate constant depended on the concentration of maleic anhydride [MA], and the linear plot of k_{decay} versus [MA] gave the second-order rate constant $k_2 = 3.2 \times 10^{10}\ M^{-1}\ s^{-1}$ for the quenching of excited (singlet) anthracene by maleic anhydride (see Fig. 4), which was in good agreement with the quenching rate constant obtained from the fluorescence measurements. On the same time scale as that of the decay of excited anthracene, the appearance and disappearance of anthracene cation-radical was observed at 720 nm (see Fig. 3(A)), and its (first-order) decay rate constant was determined to be $k = 8 \times 10^9\ s^{-1}$.

4. Discussion

Photoinduced [4 + 2] cycloaddition of anthracene to maleic anhydride and the maleimides in Chart I leads to

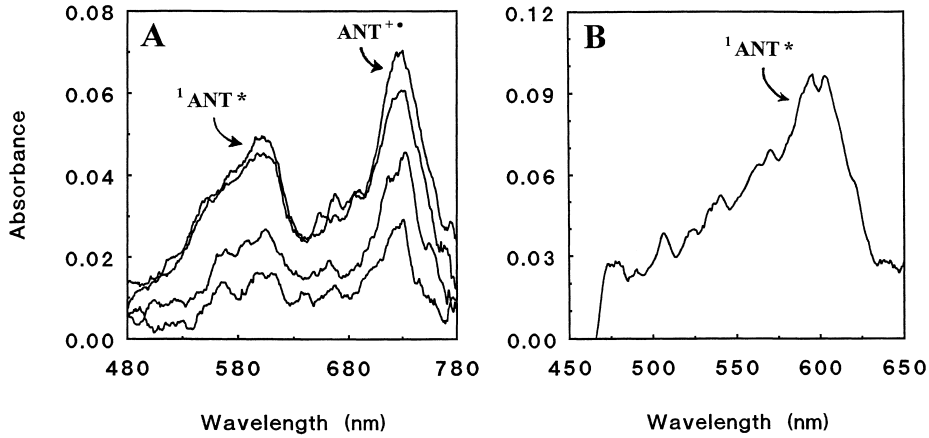

Fig. 3. (A) Concomitant decay of the absorption spectra of singlet excited anthracene (^{1}ANT*) and anthracene cation radical (ANT$^{+\bullet}$) obtained at 10, 20, 50 and 120 ps (top-to-bottom) upon 25 ps laser excitation (355 nm) of anthracene (1×10^{-4} M) in the presence of 0.3 M maleic anhydride in chloroform. (B) Absorption spectrum (S_1–S_n) of singlet excited anthracene obtained 50 ps upon 355 nm excitation of anthracene (1×10^{-4} M) in chloroform.

the Diels–Alder adducts **1–4** in high (>90%) yields. In these photoreactions, only anthracene is photoactivated by the actinic light which results in the generation of excited (singlet) anthracene (^{1}ANT*) with its distinct fluorescence emission bands and its characteristic S_1–S_n absorption spectrum (see Fig. 3(B)), i.e.

$$\text{ANT} \xrightarrow{h\nu} {}^1\text{ANT}^* \qquad (2)$$

4.1. Electron-transfer quenching of excited anthracene

The excited anthracene (^{1}ANT*) subsequently reacts with the various dienophiles in Chart I at diffusion-controlled rates (i.e. $k_2 \cong 3 \times 10^{10}\ \text{M}^{-1}\ \text{s}^{-1}$) as determined by Stern–Volmer analysis of the fluorescence quenching experiments in Fig. 2. The nature of the quenching process is revealed by the time-resolved absorption measurements with maleic anhydride as a typical example[5]. Thus, the quenching of excited anthracene by maleic anhydride leads to the formation of anthracene cation radical as a result of one-electron transfer from the electron-rich anthracene (^{1}ANT*) to the electron-poor maleic anhydride (MA) [6], i.e.

$$^1\text{ANT}^* + \text{MA} \xrightarrow{k_2 = 3\times10^{10}\ \text{M}^{-1}\text{s}^{-1}} [\text{ANT}^{+\bullet}, \text{MA}^{-\bullet}] \qquad (3)$$

This electron transfer is highly exothermic ($\Delta G_{\text{ET}} \approx -1.5$ eV)[7] which explains its diffusion-controlled rate [46]. Interestingly, the anthracene cation radical generated by electron-transfer quenching of the excited anthracene shows about the same decay rate as ^{1}ANT* itself, which points to a very short lifetime of the anthracene cation radical. In other words, the appearance and disappearance of ANT$^{+\bullet}$ follows the appearance and disappearance of ^{1}ANT*; and at completion of the quenching process all cation radicals have reacted further.

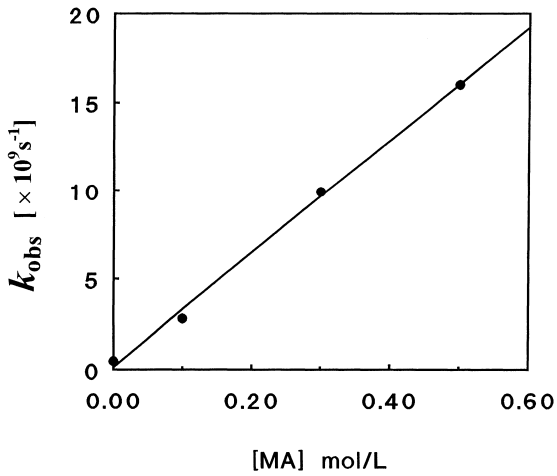

Fig. 4. Plot of the observed (first-order) rate constants of ^{1}ANT* decay vs. the maleic anhydride concentration. The slope yields a second-order quenching rate constant of $k_2 = 3.2 \times 10^{10}\ \text{M}^{-1}\ \text{s}^{-1}$.

4.2. Electron-transfer as the critical reaction step prior to cycloaddition

The observation of electron-transfer quenching of singlet excited anthracene by the dienophiles as established by fluorescence and time-resolved absorption measurements

[5] Time-resolved absorption measurements with the maleimides were unsuccessful owing to their absorption profiles which strongly overlapped with that of anthracene and thus precluded the unambiguous photoactivation of anthracene.

[6] The stoichiometry of the electron transfer demands that MA$^{-\cdot}$ is cogenerated with the anthracene cation radical ANT$^{+\cdot}$. However, the MA$^{-\cdot}$ absorption band is centered at 330 nm [42] which is outside the detection window of the 25 ps pump-probe experiments [45].

[7] According to Rehm and Weller [46], the free energy for electron transfer from an excited donor to an acceptor is determined by $\Delta G = E_{\text{ox}} - E_{\text{red}} - E_{\text{s}}$. By taking $E^{\text{p}}_{\text{ox}} \cong 0.95$ V as oxidation (peak) potential of anthracene [25], $E^{\text{p}}_{\text{red}} \cong -0.81$ V as reduction (peak) potential of maleic anhydride [47], and $E_{\text{s}} = 3.3$ V as singlet energy of anthracene [41], we calculate $\Delta G_{\text{ET}} \cong -1.5$ eV.

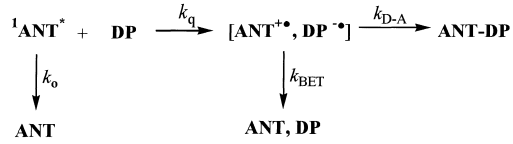

Scheme 1.

leads to the question whether this electron transfer is the critical reaction step prior to cycloaddition, or whether it is an unrelated side reaction. To answer this question, let us analyze the concentration dependence of the quantum yields (Φ_{D-A}) for Diels–Alder adduct formation in Table 2 and Fig. 1. Fig. 1(A) illustrates the asymptotic behavior of Φ_{D-A} with increasing dienophile concentration, which results in the maximum observed quantum yields of 0.013 and 0.11 for MA and PFMI, respectively. On the basis of a simple reaction scheme (Scheme 1), the overall quantum efficiency (Φ_{D-A}) for the formation of the cycloadduct ANT-DP can be expressed as the product of the quenching efficiency (Φ_Q) and the limiting cycloaddition efficiency ($\Phi_{D-A,\infty}$), i.e.

$$\Phi_{D-A} = \Phi_Q \times \Phi_{D-A,\infty} \tag{5}$$

with

$$\Phi_Q = \frac{k_q[DP]}{k_0 + k_q[DP]} \tag{6}$$

and

$$\Phi_{D-A,\infty} = \frac{k_{D-A}}{k_{D-A} + k_{BET}} \tag{7}$$

The combination of Eqs. (5) and (6) leads to a double-reciprocal relationship between the quantum yields and the dienophile concentrations which is graphically depicted in Fig. 1(B), i.e.

$$\frac{1}{\Phi_{D-A}} = \frac{1}{\Phi_{D-A,\infty}} + \frac{1}{\Phi_{D-A,\infty}}\frac{k_0}{k_q}\frac{1}{[DP]} \tag{8}$$

Thus, the intercepts of the double reciprocal plots represent the reciprocal limiting quantum yields, and the ratio between the natural singlet decay rate (k_0) and the quenching rate constant (k_q) can be extracted from the slope. From the intercepts of the double-reciprocal plots (see Section 3), we obtain 0.014 and 0.16 as limiting quantum yields for MA and PFMI, respectively, which are in good agreement with the highest obtained experimental quantum yields. Taking $k_0 = 1/\tau_0 = 4.8 \times 10^8\ s^{-1}$ (vide supra), quenching rate constants of $k_q \approx 4 \times 10^{10}\ M^{-1}\ s^{-1}$ were obtained for both dienophiles in good agreement with the diffusion-controlled quenching rate constants derived from the Stern–Volmer plots in Fig. 2 and the time-resolved absorption measurements in Fig. 4. Yet, the good agreement of the k_q values obtained from the Stern–Volmer plots (Fig. 2), the absorption measurements (Fig. 4), and the double-reciprocal plots (Fig. 1(B)) is merely necessary, but not sufficient evidence for the electron-transfer mechanism put forward in Scheme 1 since the kinetic analysis only implies that a diffusion-controlled process proceeds the cycloaddition step. Thus, additional evidence is needed to underpin the electron-transfer concept. In fact, the solvent and salt effects on the cycloaddition quantum yields provide the strongest experimental support since both effects probe the role of ions in the cycloaddition reaction sequence. Thus, polar solvents as well as inert salt in high concentrations intercept the initial ion-radical pair [ANT$^{+\bullet}$, DP$^{-\bullet}$] in Scheme 1 by either enhanced ion dissociation or by ion exchange, respectively, i.e.

$$[ANT^{+\bullet}, DP^{-\bullet}] \xrightarrow[\text{solvent}]{\text{polar}} ANT^{+\bullet} + DP^{-\bullet} \tag{9}$$

$$[ANT^{+\bullet}, DP^{-\bullet}] \xrightarrow{TBA^+PF_6^-} ANT^{+\bullet}PF_6^- + TBA^+DP^{-\bullet} \tag{10}$$

As a result, the efficiency of cycloaddition that occurs within the geminate ion-radical pair decreases substantially with increasing solvent polarity and/or addition of inert salt (see Table 3).

In summary, the fluorescence quenching experiments, the time resolved absorption measurements and the effects of solvent polarity and added salt all reveal the cation-radical pair in Scheme 1 as the critical intermediate in the photo-induced [4 + 2] cycloaddition of anthracene to dienophiles such as maleic anhydride and maleimides. As such, the observation of the ion-radical pair prior to cycloaddition represents striking experimental evidence for the polar reaction intermediate invoked in MO correlation diagrams [20–23] to accommodate for high quantum efficiencies of (otherwise) symmetry-forbidden [17–19] photocycloadditions.

Acknowledgements

We thank R. Thummel for permission to use his luminescence spectrometer, and the National Science Foundation for financial support.

References

[1] N.J. Turro, G.S. Hammond, J. Am. Chem. Soc. 84 (1962) 2841.
[2] G.O. Schenck, R. Steinmetz, Bull. Soc. Chim. Belg. 71 (1962) 781.
[3] G.O. Schenck, J. Kuhls, C.H. Krauch, Liebigs Ann. Chem. 693 (1966) 20.
[4] B.D. Kramer, P.D. Bartlett, J. Am. Chem. Soc. 94 (1972) 3934.
[5] D.P. Kjell, R.S. Sheridan, J. Am. Chem. Soc. 106 (1984) 5368.
[6] D.P. Kjell, R.S. Sheridan, J. Photochem. 28 (1985) 205.
[7] S.J. Hamrock, R.S. Sheridan, Tetrahedron Lett. 29 (1988) 5509.
[8] S.J. Hamrock, R.S. Sheridan, J. Am. Chem. Soc. 111 (1989) 9247.
[9] U. Burger, P.-A. Lottaz, P. Millasson, G. Bernardinelli, Helv. Chim. Acta 77 (1994) 850.
[10] J.P. Simons, Trans. Faraday Soc. 56 (1960) 391.
[11] D.R. Arnold, L.B. Gillis, E.B. Whipple, Chem. Commun. (1969) 918.
[12] D. Bryce-Smith, D.E. Foulger, A. Gilbert, J. Chem. Soc., Chem. Commun. (1972) 664.
[13] G. Kaupp, Liebigs Ann. Chem. (1973) 844.
[14] G. Kaupp, Liebigs Ann. Chem. (1977) 254.

[15] B. Pandey, P.V. Dalvi, Angew. Chem. Int. Ed. Engl. 32 (1993) 1612.
[16] M. D'Auria, Tetrahedron Lett. 36 (1995) 6567.
[17] R. Hoffmann, R.B. Woodward, Acc. Chem. Res. 1 (1968) 17.
[18] R.B. Woodward, R. Hoffmann, The Conservation of Orbital Symmetry, Academic Press, New York, 1970.
[19] M.J.S. Dewar, Angew. Chem. Int. Ed. Engl. 10 (1971) 761.
[20] N.D. Epiotis, R.L. Yates, J. Org. Chem. 39 (1974) 3150.
[21] N.D. Epiotis, J. Am. Chem. Soc. 94 (1972) 1924, 1941, 1946.
[22] S. Inagaki, Y. Hirabayashi, Chem. Lett. (1978) 135.
[23] D. Bryce-Smith, Chem. Commun. (1969) 806.
[24] L.J. Andrews, R.M. Keefer, J. Am. Chem. Soc. 77 (1955) 6284.
[25] S. Fukuzumi, J.K. Kochi, Tetrahedron 38 (1982) 1035.
[26] R. Sustmann, H.-G. Korth, U. Nüchter, I. Siangouri-Feulner, W. Sicking, Chem. Ber. 124 (1991) 2811.
[27] V.D. Kiselev, J.G. Miller, J. Am. Chem. Soc. 97 (1975) 4036.
[28] R. Sustmann, K. Lücking, G. Kopp, M. Rese, Angew. Chem. Int. Ed. Engl. 28 (1989) 1713.
[29] M. Dern, H.-G. Korth, G. Kopp, R. Sustmann, Angew. Chem. Int. Ed. Engl. 24 (1985) 337.
[30] G. Kaupp, R. Dyllick-Brenzinger, I. Zimmermann, Angew. Chem. Int. Ed. Engl. 14 (1975) 491.
[31] J.M. Barrales-Rienda, J. Gonzalez Ramos, M. Sanchez Chaves, J. Fluorine Chem. 9 (1977) 293.
[32] D.D. Perrin, W.L.F. Armarego, D.R. Perrin, Purification of Laboratory Chemicals, 2nd ed., Pergamon, New York, 1980.
[33] P.D. Bartlett, S.G. Cohen, J. Am. Chem. Soc. 62 (1940) 1183.
[34] W.E. Bachmann, W. Cole, J. Org. Chem. 4 (1939) 60.
[35] M. P Cava, R.H. Schlessinger, Tetrahedron 21 (1965) 3073.
[36] C.G. Hatchard, C.A. Parker, Proc. Royal Soc. 235A (1956) 518.
[37] J.G. Calvert, J.N. Pitts, Jr., Photochemistry, Wiley, New York, 1996, p. 786.
[38] T.M. Bockman, J.K. Kochi J., , J. Chem. Soc., Perkin Trans. 2 (1996) 1633.
[39] C. Reichardt, Solvent Effects in Organic Chemistry, Verlag Chemie, New York, 1979.
[40] P.J. Wagner, in: J.C. Scaiano (Ed.), Handbook of Organic Photochemistry, CRC Press, Boca Raton, FL, 1989, vol. 2, p. 267.
[41] S.L. Murov, I. Carmichael, G.L. Hug, Handbook of Photochemistry, Marcel Dekker, New York, 1993, p. 7.
[42] T. Shida, Electronic Absorption Spectra of Radical Ions, Elsevier, New York, 1988, p. 69.
[43] S.M. Hubig, J.K. Kochi, J. Phys. Chem. 99 (1995) 17578.
[44] J.M. Masnovi, J.K. Kochi, E.F. Hilinski, P.M. Rentzepis, J. Phys. Chem. 89 (1985) 5387.
[45] S.M. Hubig, M.A.J. Rodgers, in: J.C. Scaiano (Ed.), Handbook of Organic Photochemistry, CRC Press, Boca Raton, FL, 1989, vol. I, p. 319.
[46] D. Rehm, A. Weller, Isr. J. Chem. 8 (1970) 259.
[47] D.-L. Sun, unpublished results.